Solution Synthesis of Metal-Oxide Films

Pulsed Laser Assisted Polycrystalline Growth of Oxide Thin Films for Efficient Processing

Tomohiko Nakajima, Kentaro Shinoda and Tetsuo Tsuchiya
Flexible Chemical Coating Group, Advanced Manufacturing Research Institute, National
Institute of Advanced Industrial Science and Technology, Tsukuba Central 5, 1-1-1 Higashi,
Tsukuba, Ibaraki, 305-8565, Japan

ABSTRACT

We have investigated the polycrystalline growth by means of an excimer laser assisted metal organic deposition process and the strategy for the efficient growth. It was revealed that the pulsed photo thermal heating properties must be controlled by changing the laser fluence according to the substrate properties, such as thermal diffusivity. The threshold of the t_{eff} value for initial crystal nucleation is approximately 70 ns for oxide thin films. For the fabrication of good quality films with high crystallinity and without a laser ablation of the film surface, it is necessary that the irradiated laser fluence is adjusted to the conditions of t_{eff} (efficient annealing time) > 70 ns and T_{max} (maximum temperature) < T_m (melting point). Obtained oxide films by using the pulsed UV laser has large crystallite size, and it well functioned to enhance physical properties of films. For further efficient growth for polycrystalline growth of the oxide films, the starting solution containing nanoparticles is very useful: it is named as photo-reaction of nanoparticles process.

INTRODUCTION

Numerous inorganic materials which have been investigated for future electronics devices are usually incorporated in the devices as thin films. There are two main requirements for film growth methods for future applications: (1) Efficient fabrication for lower cost, and (2) low temperature operation for substrates which cannot withstand high temperatures ($T > 500$ °C). It is now widely accepted that chemical solution deposition (CSD) methods, such as a metal organic deposition (MOD) [1,2] and sol-gel [3,4] processes are better than physical and chemical vapor deposition processes in terms of process simplicity and low cost. However, the application of CSD as a conventional heating process is also an issue for low temperature fabrication, and is generally limited by the heat resistance properties of the substrate. To resolve this problem, we have developed processes by means of a combination of CSD and ultraviolet (UV) irradiation [5–8]. We have investigated a new method to fabricate oxide thin films at low temperatures using an advanced conventional MOD process, wherein oxide films are crystallized by means of excimer laser irradiation ($\lambda = 193$, 248, and 308 nm) instead of high temperature furnace heating in the MOD process [9]. We have named this process as an excimer laser-assisted metal organic deposition (ELAMOD).

Thus far, we have demonstrated that not only polycrystalline films but also epitaxial films of oxide materials can be grown by ELAMOD, when a single crystal substrate has a small lattice mismatch with the film [9,10]. In these studies, we noticed that crystal growth of oxide films under UV laser irradiation in the CSD process cannot be interpreted by only a photo-thermal heating effect [7,10]: some photo-chemical reaction at growth interface should be taken into account to the crystal growth mechanism in this process. Concerning the polycrystalline growth

3

of oxide thin films, we mainly focused on the controlling parameters which affect an initial nucleation on amorphous and/or polycrystalline substrates [11]. In this paper, we investigate that key techniques for efficient polycrystalline growth under pulsed UV laser irradiation in the ELAMOD and recent developed photo-reaction of nanoparticles (PRNP) processes [12,13].

EXPERIMENT

For preparations of polycrystalline oxide thin films by means of the ELAMOD in this study, the starting solution was firstly prepared by mixing solutions of fatty acid salts dissolved in organic solvents including the constituent metals to obtain the required concentration and viscosity for spin coating. The prepared solution was spin-coated onto amorphous glass substrates at 4000 rpm for 10 s. The coated films were dried at 100 °C in air to remove the solvent, and then heated to 400 °C in air for 10 min to decompose the organic components of the films. The preheated films were irradiated with a KrF laser using a Compex110 Lambda Physik at pulse duration of 25 ns in air. The laser energy was homogenized by a beam homogenizer in 7 x 7 mm^2 area. The structural properties of the films were studied by a SmartLab RIGAKU X-ray diffractometer with Cu K_α radiation, $V = 40$ kV, and $I = 30$ mA. The cross-sectional transmittance electron microscopy (XTEM) was carried out using a JEM-2010 JEOL instrument operating at 200 kV. Temperature variations during the laser irradiation process can be described by the heat diffusion equation simplified into a one-dimensional heat flow as follows [10]:

$$\rho C \frac{\partial T}{\partial t} = \kappa \frac{\partial^2 T}{\partial z^2} + \alpha I(z,t)$$

where T is the temperature function of time t and depth z, ρ is the mass density, C is the specific heat capacity, α is the optical absorption coefficient, κ is the thermal conductivity, and the $I(z,t)$ is the laser power density. The laser power $I(z,t)$ is given by:

$$I(z,t) = I_0(t) \cdot (1-R) \cdot \exp(-\alpha z)$$

where R is the reflectivity, and $I_0(t)$ was described as a smooth pulse approximated by:

$$I_0(t) = I_0 \cdot \left(\frac{t}{\tau}\right)^\beta \cdot \exp\left(\beta\left(1-\frac{t}{\tau}\right)\right)$$

where I_0 is the incident pulse power density, τ_0 is the pulse duration, and β determines the temporal pulse shape. We carried out numerical simulations for the temperature variations for the excimer laser annealing process by means of a difference approximation based on the above mentioned equations.

DISCUSSION

For searching good conditions to make polycrystalline thin films in the ELAMOD process, we have to take into account photo-thermal heating profiles for first nucleation in the

4

precursor matrix. Firstly, we can evaluate photo-thermal heating under a UV laser pulse by using the one dimensional heat flow model described above. Figure 1 shows the representative pulsed temperature rise and decay curve under the UV laser irradiation.
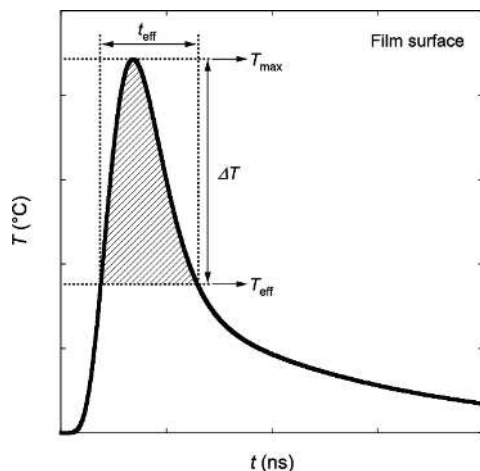

Figure 1. Schematic simulated temperature variation curve at precursor film surface under a UV laser irradiation by using a one dimensional heat flow. T_{max}, T_{eff}, and t_{eff} represent maximum temperature, effective temperature for crystallization and effective time for crystallization, respectively. The T_{eff} is a temperature in which the x-ray diffraction intensity can be detectable after furnace heating for 1h, this means nucleated nanodomains successfully emerged in the matrix. The t_{eff} is a time over the T_{eff}. The ΔT equals to $T_{max}-T_{eff}$.

Optimum conditions of laser irradiation are firstly chosen by keeping t_{eff} above 50–70 ns. This value has been obtained by precise control of t_{eff} and ΔT in the preparation of perovskite manganite thin films on glass substrates. The contour map for x-ray diffraction intensity of LaMnO$_3$ thin films after the KrF laser irradiation to the precursor with 1000 pulses at room temperature is shown in Fig. 2. The t_{eff} and ΔT were controlled by changing thermal diffusion property. The detailed conditions are shown in the previous literature [11].
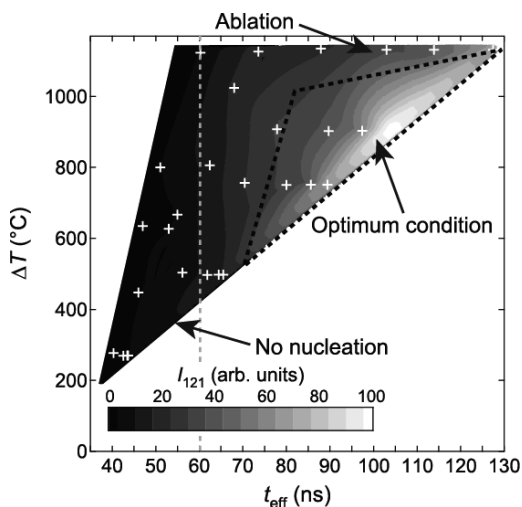
5

Figure 2. Contour map for the t_{eff} and ΔT dependence of the 121 peak intensities of LaMnO$_3$ thin films. White crosses indicate the observed points. T_{max} and T_{eff} in this system were 1920 °C and 790 °C, respectively [11].

As seen in this figure, there is clear threshold at around t_{eff} = 60 ns for the nucleation of LaMnO$_3$ nanodomains in the precursor matrix. Best condition for the polycrystalline growth was located above t_{eff} = 110 ns and at around ΔT = 850 °C. Above ΔT = 1000 °C, the crystallinity was reduced because the laser ablation would occur near melting point (T_m) of LaMnO$_3$ at 1900 °C. Thus, this result leads to a following conclusion: for an efficient polycrystalline growth from the amorphous LaMnO$_3$ matrix, it was revealed that the pulsed photothermal heating properties must be controlled by changing the laser fluence according to the substrate properties, such as thermal diffusivity. The threshold of the t_{eff} value for initial crystal nucleation is approximately 60 ns for this material. For the fabrication of good quality films with high crystallinity and without a laser ablation of the film surface, it is necessary that the laser fluence is adjusted to the conditions of t_{eff} > 90 ns and 500 °C < ΔT < 1000 °C. About the other materials, optimum t_{eff} values for the RbLaNb$_2$O$_7$ and CaTiO$_3$ were determined as *c.a.* 160 ns and 200 ns, respectively [14,15]. The thresholds of t_{eff} for nucleation of these materials were *c.a.* 70 ns. Therefore, we thought that these key parameters have universality to some extent in many oxide materials.

The notable feature of the polycrystalline growth under the laser irradiation is that crystallite size significantly increases if the laser irradiation conditions are optimized. This characteristic is linked to the epitaxial growth picture in the ELAMOD process. Under UV laser irradiation, the materials can be epitaxially grown on the crystal seed if it has similar crystal lattices with objective materials: it is strongly enhanced by photo-chemical effect at the reaction interface. In polycrystalline growth under the pulsed UV laser, first nucleation sites emerged by photo-thermal heating act as a seed, followed by a rapid succeeding crystal growth

6

homoepitaxially from them enhanced by the abovementioned photo-chemical effect. Finally, the laser irradiation process can prepare highly crystalline oxide thin films with large grain size.

Figure 3(a) shows a XTEM image for a $CaTiO_3$ polycrystalline thin film on a glass substrate prepared by the ELAMOD process using a KrF irradiation at a fluence of 100 mJ/cm^2 for 5000 pulses and at 100 °C in air. The film thickness was evaluated to be *c.a.* 100 nm. Noteworthy is that it had very large grain size compared to the films which are usually obtained by conventional heating process: it was a single crystal in out-of-plane direction and has around 700 nm grains along the in-plane direction. Figures 3(b) and 3(c) show high-resolution XTEM images for each crystal grain. Both images clearly exhibit the grains are single crystal along the depth direction. The inset of Fig. 3(b) is the selected area electron diffraction (SAED) at the whole region of one grain shown in the Fig. 3(b). The SAED pattern was derived only from [111]-plane, indicating that it was evidently single crystal.
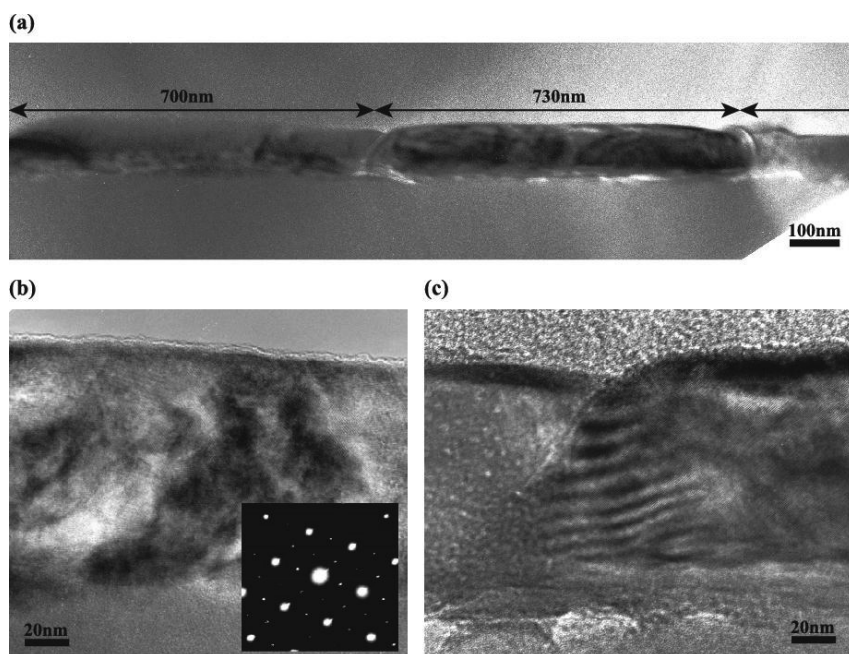

Figure 3. (a) Bright field image for the $CaTiO_3$ thin film. Arrows indicate each grain. (b,c) High resolution XTEM images. The inset of (b) shows the SAED pattern collected from the whole region of the grain.

Based on the polycrystalline growth picture and the characteristics in the ELAMOD process, we focus on a method for an efficient polycrystalline growth by using the pulsed UV laser. It is a use of nanoparticles as a seed into a starting solution. Actually, the first nucleation

from an amorphous precursor matrix under the pulsed UV laser usually needs more than 1000 pulses. If a starting solution contains objective nanoparticles, the continuing crystal growth would rapidly occur. By means of this method called as PRNP, we have already efficiently prepared oxide thin films such as ITO and WO_3 [12,13]. For the preparation of WO_3 thin films, we used an alcohol solution contains WO_3 nanoparticles with the particle size at around 5–30 nm as shown in Fig. 4(a). The starting solution was deposited onto glass substrates by spin coating, then the particles coated substrate was irradiated by KrF laser at a fluence of 50 mJ/cm^2 for 7500 pulses at room temperature. For a comparison, precursor film was also treated by furnace heating at 500 °C for 60 min in air. Figure 4(b) shows the XTEM for the heat treatment sample. The crystallite size was similar with original particles. Conversely, it was much increased especially at near film surface prepared by the laser irradiation as shown in Fig. 4(c). The crystallites near the film surface were significantly larger, up to 70 nm, and their size gradually decreased as the depth increased. This is due to photo-thermal temperature decay from the surface.
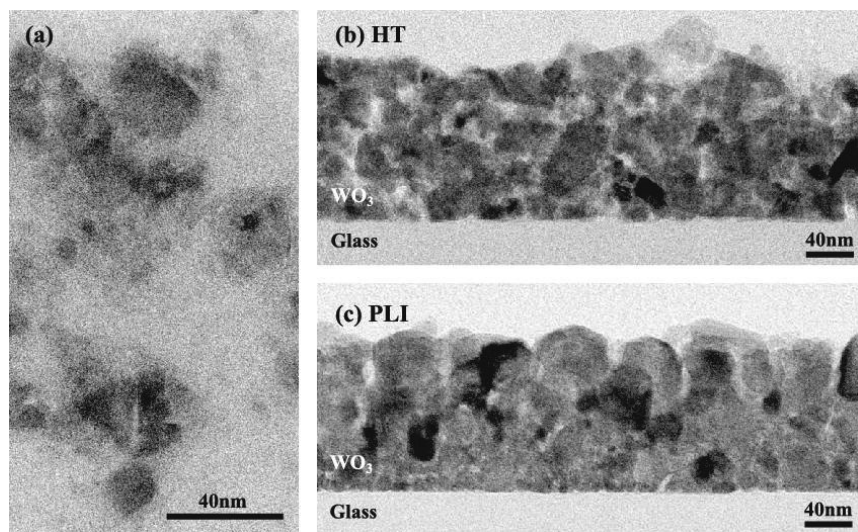

Figure 4. (a) Original WO_3 nanoparticles in the starting solution for the PRNP process. The prepared WO_3 thin films by means of (b) furnace heating (HT) at 500 °C and (c) pulsed laser irradiation (PLI) at a fluence of 50 mJ/cm^2 at room temperature.
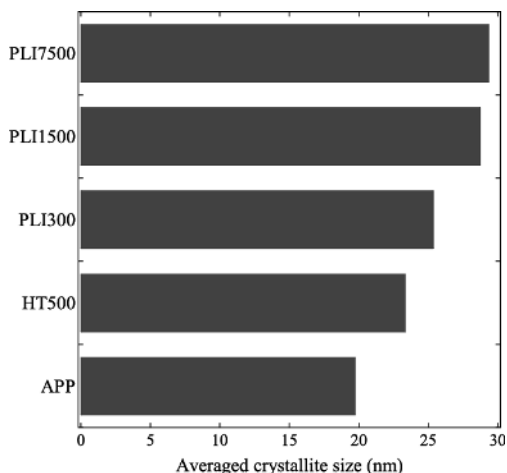
Figure 5. Calculated averaged crystallite size for the WO_3 as-prepared particles (APP) and thin films by heat treatment at 500 °C (HT500) and PRNP (PLI300, PLI1500 and PLI7500).

The averaged crystallite size of the samples prepared by heat treatment at 500 °C (HT500) and PRNP for 300 pulses (PLI300), 1500 pulses (PLI1500) and 7500 pulses (PLI7500) were evaluated by X-ray diffraction using Scherrer's equation (Fig. 5) [16]. By only 300 pulses irradiation, the averaged crystallite size exceeded that of heat treatment one. Then, it was saturated at around 1500 pulses. This indicates that the necessary pulse number for sufficient polycrystalline growth can be much reduced by introducing nanoparticles into a starting solution, leading a further cost-friendly process.
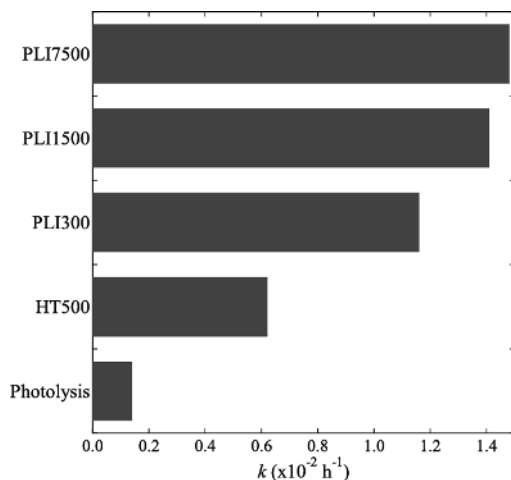
9

Figure 6. The rate constant for the photocatalytic degradation of methylene blue for the WO_3 thin films by heat treatment at 500 °C (HT500) and PRNP (PLI300, PLI1500 and PLI7500). Photolysis means a blank measurement.

The large crystallite growth under the pulsed UV laser irradiation as shown in Figs. 4 and 5 would be good for the physical properties of the films, which is especially related to electron transfer. Figure 6 shows the photocatalytic degradation rate constant (k) of methylene blue in aqueous solution for the prepared WO_3 thin films in which the surface was grafted by Cu(II) for enhancement of photocatalytic activity under visible light irradiation using Xe lamp at 100 kLux through a UV cut-off filter ($\lambda > 400$ nm). The k value was clearly increased by laser irradiation compared to the sample prepared by heat treatment. The surface crystallinity which depends on sufficient crystallite growth in WO_3 thin films was greatly improved by pulsed laser irradiation in the PRNP process. The enhanced crystallinity would stimulate the photoexcited electron/hole transfer at the film surface, resulting in the improvement of the photocatalytic activity. This kind of origin was also observed a transparent conducting material ITO prepared by the PRNP process, suggesting that the enhanced crystallite growth by means of the pulsed laser irradiation is efficient for enhanced physical properties of polycrystalline oxide thin films.

CONCLUSIONS

We have investigated the polycrystalline growth by means of the ELAMOD process and the strategy for the efficient growth. It was revealed that the pulsed photo thermal heating properties must be controlled by changing the laser fluence according to the substrate properties, such as thermal diffusivity. The threshold of the t_{eff} value for initial crystal nucleation is approximately 70 ns for oxide thin films. For the fabrication of good quality films with high crystallinity and without a laser ablation of the film surface, it is necessary that the irradiated

10

laser fluence is adjusted to the conditions of $t_{\text{eff}} > 70$ ns and $T_{\text{max}} < T_{\text{m}}$. Obtained oxide films by using the pulsed UV laser has large crystallite size, and it well functioned to enhance physical properties of films. For further efficient growth for polycrystalline growth of the oxide films, the starting solution containing nanoparticles enables to stimulate the growth rate: it is named as PRNP process.

REFERENCES

1. A. C. Westerheim, P. C. Mcintyre, S. N. Basu, D. Bhatt, L. S. Yujahnes, A. C. Anderson and M. J. Cima, J. Electron. Mater. **22**, 1113 (1993).
2. T. Mihara, H. Yoshimori, H. Watanabe and C. A. P. Araujo, Jpn. J. Appl. Phys. **34**, 5233 (1995).
3. D. Avnir, V. R. Kaufman and R. Reisfeld, J. Non-cryst. Solids **74**, 395 (1985).
4. C. J. Brinker, A. J. Hurd and G. C. Frye, J. Non-cryst. Solids **121**, 294 (1990).
5. T. Nagase, T. Ooie and J. Sakakibara, Thin Solid Films **357**, 151 (1999).
6. T. Tsuchiya, A. Watanabe, Y. Imai, H. Niino, I. Yamaguchi, T. Manabe, T. Kumagai and S. Mizuta, Jpn. J. Appl. Phys. **38**, L823 (1999).
7. S. C. Lai, H-T. Lue, K. Y. Hsieh, S. L. Lung, R. Liu, T. B. Wu, P. P. Donohue and P. Rumsby, J. Appl. Phys. **96**, 2779 (2004).
8. C. S. Sandu, V. S. Teodorescu, C. Ghica, B. Canut, M. G. Blanchin, J. A. Roger, A. Brioude, T. Bret, P. Hoffman and C. Garapon, Appl. Surf. Sci. **208–209**, 382 (2003).
9. T. Tsuchiya, T. Yoshitake, Y. Shimakawa, I. Yamaguchi, T. Manabe, T. Kumagai, Y. Kubo and S. Mizuta, Jpn. J. Appl. Phys. **42**, L956 (2003).
10. T. Nakajima, T. Tsuchiya, M. Ichihara, H. Nagai and T. Kumagai, Chem. Mater. **20**, 7344 (2008).
11. T. Nakajima, T. Tsuchiya, M. Ichihara, H. Nagai and T. Kumagai, Appl. Phys. Express **2**, 023001 (2009).
12. T. Tsuchiya, F. Yamaguchi, I. Morimoto, T. Nakajima and T. Kumagai, Appl. Phys. A **99**, 745 (2010).
13. T. Nakajima, T. Kitamura and T. Tsuchiya, Appl. Catal. B **108–109**, 47 (2011).
14. T. Nakajima, T. Tsuchiya and T. Kumagai, Appl. Phys. A **93**, 51 (2008).
15. T. Nakajima, T. Tsuchiya and T. Kumagai, Cryst. Growth Des. **10**, 4861 (2010).
16. L. V. Azaroff, Elements of X-ray Crystallography, McGrawHill, New York (1968).